



UNIVERSITY OF TWENTE.

Faculty of Engineering Technology

Internship Report

3D Printing - Depowdering techniques

Zuhair Siddiqui - s1705180

January 20, 2017

Prepared for:

Dr Ir. Maurice Limpens

TNO

Dep. EFAM

5612 AH Eindhoven

The Netherlands



TNO report

| Final report

De Rondon 1
5612 AP Eindhoven
P.O. Box 6235
5600 HE Eindhoven
The Netherlands

www.tno.nl

T +31 88 866 50 00
F +31 88 866 88 19

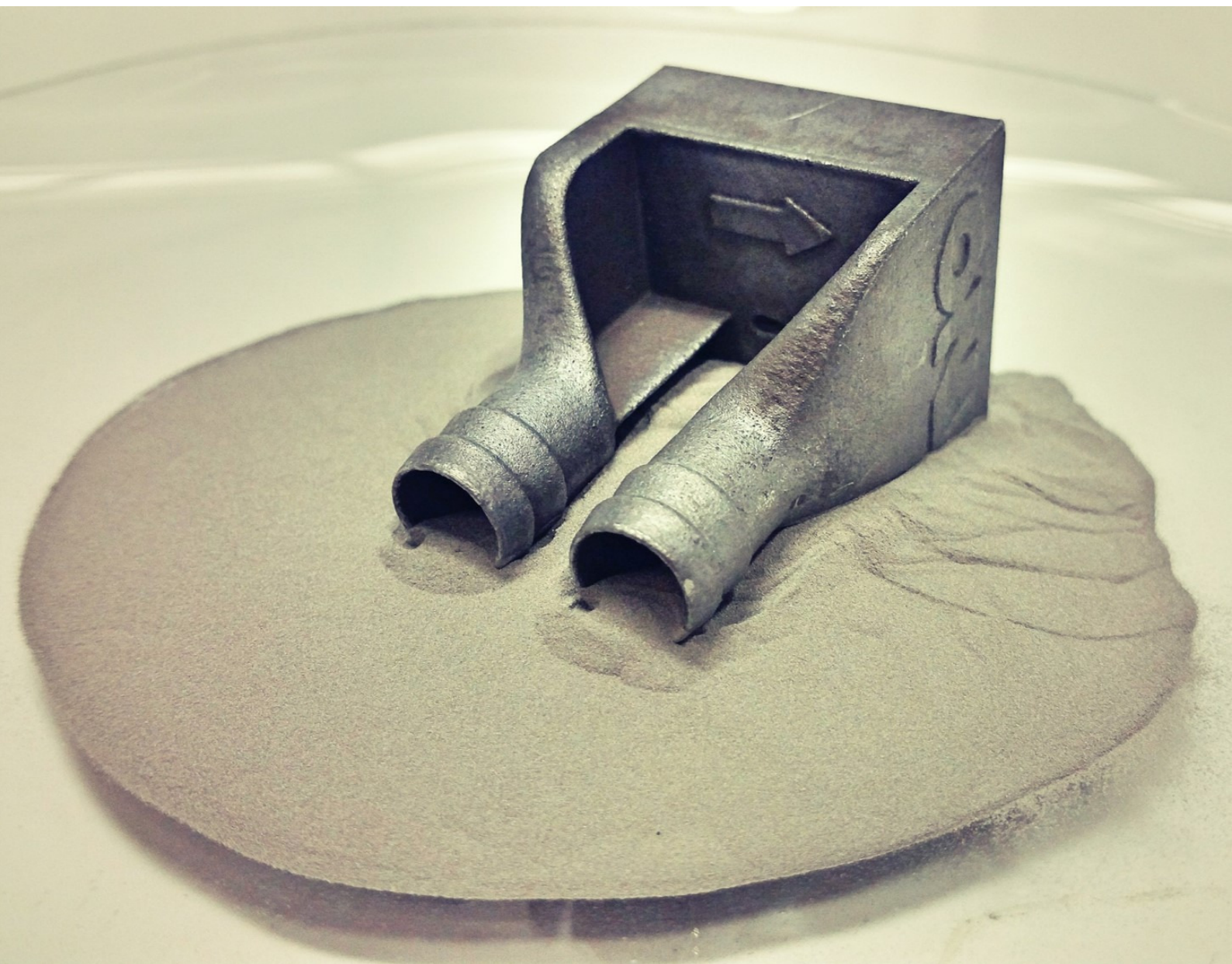
Date	20 January 2017
Author(s)	Zuhair Siddiqui
Copy no	
No. of copies	
Number of pages	53 (incl. appendices)
Number of appendices	2
Sponsor	
Project name	WP3.34 Post processing
Project number	060.12510/01.03.03

All rights reserved.

No part of this publication may be reproduced and/or published by print, photoprint, microfilm or any other means without the previous written consent of TNO.

In case this report was drafted on instructions, the rights and obligations of contracting parties are subject to either the General Terms and Conditions for commissions to TNO, or the relevant agreement concluded between the contracting parties. Submitting the report for inspection to parties who have a direct interest is permitted.

© 2017 TNO



Acknowledgment

I would like to first express my gratitude to TNO for allowing me to do an internship at the Equipment for Additive Manufacturing (EFAM) division and allowing me to make use of the knowledge and resources.

I would like to thank Dr. ir. Maurice Limpens for his never-ending support during the internship. I would like to also thank Dr. ir. Erwin Meinders for giving me the chance to be part of EFAM and also Elma Janssen for her support in the beginning during the security clearance. The review and feedback received from the peers also aided in successful completion of the project.

Furthermore, I would like to thank Dr. Theo van der Meer (UTwente) for his support, without which I would not be able to do this internship in the first place. Additionally I would like to thank Edwin van dan Eijnden, Ruud Olieslagers, John Werftt and Bob Onderdelinden, Hartmut Fischer, Hessel Maalderink, Henk Buining and Margot Segers.

Preface

The aim of this report is to determine if it is possible to completely depowder a 3D printed structure. In Selective Laser Melting, the metal parts are built layer-by-layer. A roller spreads out the powder onto the bed where a high powered laser then melts the parts together. The roller spreads a layer again and the process is repeated until the print-job is completed. Due to layer by layer construction of metal part, powder not melted by laser will become part of the structure. Conventional techniques (blow drying and using hands to brush off) have proven to be insufficient means to depowder the structure efficiently, especially structures with internal dead spaces or complex geometries that are hard to clean by physical means. An experiment is done to determine how the powder flows out of such structures under different orientations. The experimental results are compared with a simulation model being developed by Maurice Limpens. Then existing cleaning techniques such as laser shockwaves cleaning, ultrasounds, vibrations and chemical flushing are investigated and an additional concept of electromagnetism is presented for future scope. Furthermore, vast literature is available for cleaning of "thin-plates" via above existing methods, but have yet to be proven efficient for complex structures. Finally, the cleaning technique with most potential is selected and is checked via experiments.

Contents

Acknowledgment	i
Preface	ii
1 Executive Summary	1
2 Introduction	3
3 Powder Flow	6
3.1 Aluminum Pixel (AlSi10Mg)	6
3.2 Results	9
3.3 Conclusion	10
4 Cleaning Techniques	13
4.1 Depowdering Techniques	14
4.1.1 Laser Shockwave Cleaning	14
4.2 Electromagnetism	15
4.3 Chemical flushing	16
4.4 Vibrations and gravity	17
4.5 Ultrasonic Cleaning	17
4.6 Final selection of cleaning technique	18
5 Ultrasonic cleaning	21
5.1 Ultrasonic cleaning of the samples	22
5.2 Experimental Procedure	26
5.3 Results from ultrasonic cleaning	27
5.3.1 Stainless steel cooling jackets	27
5.3.2 Aluminum alloy pixel (AlSi10Mg)	30
5.3.3 Stainless steel pipe fitting	31
5.3.4 Stainless steel metal plate A15 and A16	32
5.4 Equipment for Imaging	35
5.4.1 Light Microscopy	35
5.4.2 Scanning Electron Microscope	35
5.4.3 Acoustic Imaging	36
5.5 Measuring angle of repose	38
5.5.1 Angle Of Repose	38
6 Discussion and Conclusion	39
7 Recommendations	40
References	41
8 Appendice	42
Appendix A Equipment Used	42
Appendix B Measuring angle of repose	44

List of Figures

1	SLM	3
2	Complex 3D printed manifold	4
3	Aluminum Pixel (AlSi10Mg).	6
4	Section view of Aluminum Pixel (AlSi10Mg) with internal features.	7
5	Experimental Setup for Powder flow	8
6	Percentage powder removed over the angle orientation.	9
7	Depiction of Aluminum pixel at 120°	10
8	Depiction of Aluminum pixel at 180°	11
9	Laser Shockwave Cleaning	14
10	Electromagnetism Schematics	15
11	Electromagnetic field Schematics	16
12	Ultrasonic Cleaning Schematics	18
13	Decision Parameters	19
14	Summary of Cleaning techniques	20
15	Acoustic frequency scale and selected applications	21
16	Branson Ultrasonic bath	22
17	Modified Ultrasonic Bath	23
18	Stainless steel cooling jacket	24
19	Aluminum alloy pixel AlSi10Mg	24
20	Stainless steel pipe fitting	24
21	Stainless steel plate A15	25
22	Conventional hex nut	25
23	Conventional stainless steel metal plate	25
24	Conventional stainless steel bolt nut	25
25	Stainless steel cooling jacket schematics	28
26	Removed powder over bubble	30
27	Powder removed	30
28	Cross-section view of Aluminum pixel	31
29	Ultrasonic cleaning results	34
30	Optical Light Microscope	35
31	Quanta 600 Scanning Electron Microscopy	36
32	Sonix ECHO™	36
33	SEM of powder	37
34	SEM of stainless steel cooling jacket	37
35	SEM of stainless steel cooling jacket and A15	38
36	Measuring the height	38
B.1	Angle of repose.	44

List of Tables

1	Summary of occupancy of the sample volume	7
2	Summary of the powder flow via respective methods	11
3	Ultrasonic cleaning of stainless steel cooling Jacket	28
4	Ultrasonic cleaning of conventional stainless steel Hex nut	29
5	Ultrasonic cleaning of conventional metal stainless steel plate	29
6	Ultrasonic cleaning of conventional stainless steel bolt nut	29
7	Ultrasonic cleaning of Aluminum pixel (AlSi10Mg)	31
8	Ultrasonic cleaning of stainless steel pipe fitting	32
9	Ultrasonic cleaning of metal stainless steel A15	32
10	Ultrasonic cleaning of metal stainless steel A16	33
A.1	Mettler Toledo XS 104 Specs	42
A.2	Mettler Toledo AE 160 Specs	42
A.3	Haraeus T6120 Oven	42
A.4	Bransonic Ultrasound RK 255 H	43
A.5	Sonix Echo	43
B.6	Angle of repose	44

List of acronyms

CAD	Computer-Aided Design
CCW	Counterclockwise Direction
CW	Clockwise Direction
LSC	Laser Shockwave Cleaning
NDT	Non-Destructive Testing
SEM	Scanning Electron Microscopy
SLM	Selective Laser Melting

1 Executive Summary

Additive manufacturing is a technology that has broken conventional manufacturing barriers. Simple to complex structures such as a screw or a mechanical turbine, can be simply drafted in Computer-Aided Design (CAD) and ultimately be "printed" for functional use. The freedom to print any complex shape favors additive manufacturing over conventional methods of manufacturing. Current additive manufacturing allows the possibilities for: Organ printing, electronics, food, metal, ceramics and plastics printing.

In the Selective Laser Melting (SLM), the structure is built or printed through spherical particles of powder that typically lie in the micron-sized range. The laser sinters (melts) the powder together to form a final shape. Naturally, not all the powder is used to print the structure, but instead used as a base or support for the next successive layer during the printing process. Thus, once the printing process is complete, the powder present within the structure becomes part of the internal structure. These small particles can clog small precise orifices, channels' and any opening within the structure. This would defeat the purpose, for instance, the functionality of a printed heat exchanger which has loose internal powder, in terms of fluid flow and heat exchange. Therefore, there is a need to have a completely powder-free internal structure, from the manufacturing perspective and the clientele requirement.

The main aim of this report is to determine how to efficiently remove excess powder from a 3D printed structure. To do this, experiments are first conducted to see if the loose powder would completely flow out of a structure at different orientations. The results of the experiments are then compared with the Simulation model developed by Maurice Limpens. The experiment was not able to depowder the structure completely whereas in the simulation the structure completely depowders. The main differences (namely interlocking, frictional forces and free flow of the powder) between experimental and simulated results are due to the fact that the latter assumes an ideal behavior of powder flow.

Since the initial goal of depowdering was not successfully met with previous experiments, current available techniques for complete cleaning are then investigated. These techniques are (but not limited to): Laser Shockwaves Cleaning, Ultrasound, Gravity and Vibrations, and Electromagnetism. Ultrasound was chosen as the mode for cleaning, since among all the available techniques ultrasound shows promising evidence of cleaning. The results from the cleaning experiment does in fact prove complete cleaning of the structure. Ultrasounds may require long cleaning hours (more than 24 hours) before the structure is completely clean. Different cleaning combinations and sequences (for instance, extreme manual tapping and shaking of the structure followed by water flushing ultimately placed under ultrasounds) drastically reduce the time required under ultrasounds. Within the scope of this report, the depowdering of 3D printed metals is prioritized.

Furthermore experiments should be conducted with various geometries and different material structures in order to obtain improved results for better agreement between simulated and experimental results. The simulation can incorporate the real flow behavior of powder (effects of

interlocking and friction) while experiments can be improved by adding excitation effects to see how it influences the powder flow. With regards to complete cleaning, other cleaning techniques can be investigated to see how they compare with ultrasounds. Additional understanding on how each respective structure (build geometry, type of metal, shapes) behave under the influence of ultrasound waves is needed. Last but not the least, freshly 3D printed structures should be used to obtain excellent depowdering results for real life practical applications.

2 Introduction

Technological advancements in additive manufacturing have allowed the freedom to create shapes and structures that were not possible before by conventional methods such as casting, milling and injection molding to name a few. Using additive manufacturing techniques, structures with complex internal geometries with thin walls and/or hidden channels can be created for use. Currently there are different industries involved in 3D printing such as: plastics, ceramics, food, and electronics, biomedical and metal.

During Selective Laser Melting (SLM) powder is added to the powder bed during the additive manufacturing to build a 3D structure. A roller spreads a layer of powder in the powder bed. A high powered laser then melts user defined regions of the powder bed to form the desired structure. The roller then reapplies fresh layer of powder over the previous printed layer. The process is repeated until the print-job is complete. The process is depicted in Figure 1. Naturally there is loose unused powder inside the empty spaces of the product at the end of the manufacturing process. Primarily, this powder is used as support during the build for the successive print layers. This powder must be removed before the structure becomes usable.

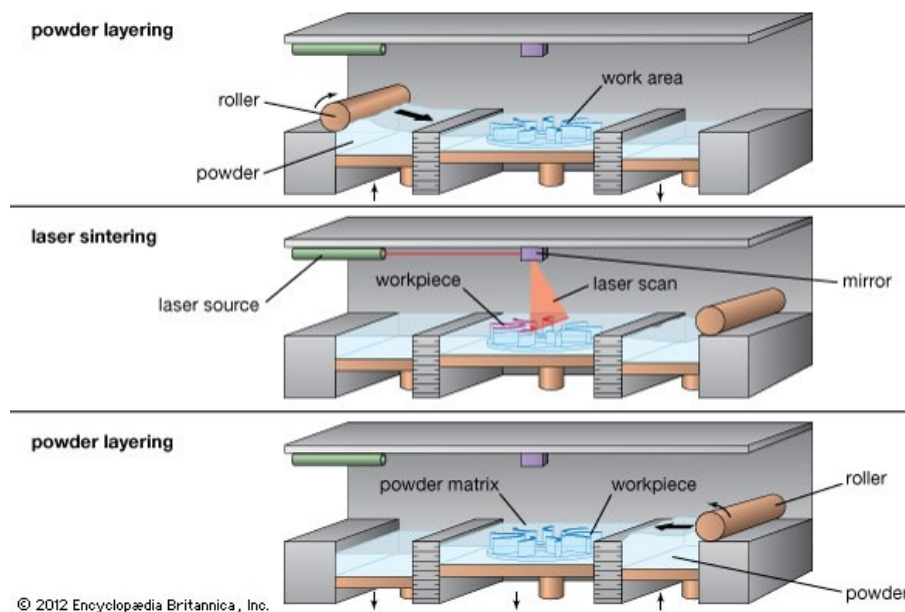


Figure 1: Depiction of steps in Sinter Laser Melting (SLM) (Britannica, 2017).

The main aim of this report is to investigate whether such 3D printed structure can be successfully depowdered to achieve a usable product. Conventional methods of cleaning a 3D printed structure during the post-processing involve blowing compressed/vacuum dry air, chemical flushing or simply brushing off the excess powder. The challenge arises when you have geometry that has internal minuscule openings or channels that have internal dimensions in the range of millimeters to micrometers, in various shapes where manual cleaning is not possible. Such an example can be seen in Figure 2 where complex manifolds can be seen.

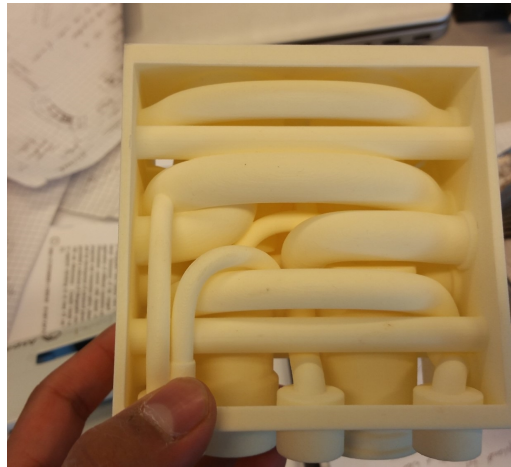


Figure 2: 3D printed manifold with complex channels

Compared to conventional manufacturing methods, additive manufacturing requires additional post processing before the final product is functional. Post processing requires additional time. Ideally cleaning techniques that do not exceed the production time is desired. At the same time, there is high demand on cleanliness for specific products (heat exchangers) by certain customers, thus accentuates the need for depowdering.

This is done first by checking whether a structure can simply be depowdered by subjecting it under different orientations. At TNO, a simulated model for depowdering a structure under different orientations is being developed by Maurice Limpens. The results of the simulation are going to be validated with experimental results.

Secondly, existing powder removal or cleaning techniques are studied to determine the efficient method for complete depowdering/cleaning of the structure. There are numerous possibilities for removal of powder, namely Laser Shockwave Cleaning (LSC), ultrasound cleaning, and powder removal under the influence of gravity and vibrations. Each technique is unique in its application. The respective cleaning techniques require extensive knowledge and expertise on the working principles of cleaning and the dynamics of powder removal. Out of the possibilities mentioned, the technique with high evidence of potential for cleaning is selected since all the techniques cannot be investigated in the duration of the internship.

As far as the scope of this internship is concerned, the depowdering techniques investigated are primarily focused on metals that are used in Selective Laser Melting (SLM), such as Stainless Steel (LPW-316), Aluminum alloys (AlSi10Mg) and Titanium alloys (Ti-6Al-4V).

Ideally, freshly 3D printed samples should be used for checking the level of cleanliness achievable from the ultrasound waves. TNO does not produce or manufacture 3D printed metal samples. Rather the metal material parts and samples are delivered by external manufacturer specializing in 3D printing, namely NLR¹ and ASML². Requesting new single customized complex samples

¹Nederlands Lucht- en Ruimtevaartcentrum (NLR) is Dutch aerospace industry involved in SLM

²ASML Holdings, a Dutch company and world's largest supplier of photolithography systems

from NLR is too expensive unless ordered in batches. Moreover it would take roughly about a month to receive a sample. Regardless, the available printed samples will be used for the purpose of experiments.

3 Powder Flow

This chapter describes the first approach to depowdering a structure at different orientations. At TNO, a simulation model is being developed by Maurice Limpens to determine whether a filled structure could be depowdered or cleaned. A simple experiment is devised where a metal sample is subjected to different orientations. The simulation results are then compared with the experimental results.

3.1 Aluminum Pixel (AlSi10Mg)

Before the experiment is setup, it is important to discuss the features of the Aluminum Pixel (AlSi10Mg). First of all, one is tempted to assume the internal geometry of the sample to be symmetrical in nature. However this is not true. The section view of Aluminum pixel can be seen in Figure 4. The Aluminum pixel is primarily to be used as cooling channel. The arrows embedded on the Aluminum pixel (as seen in Figure 3) denote the direction of the flow of any fluid, i.e. the right channel is the entrance and the left channel is the exit. The inlet channel is relatively larger than the exit channel where orifices are present. This can be seen in Figure 4.



Figure 3: Aluminum Pixel (AlSi10Mg).

Secondly, since the sample is going to be filled manually with powder it is important to know how much powder volume can be filled. According to the CAD file of the Aluminum pixel the internal volume of the structure should be roughly around $8,3 \text{ cm}^3$. To confirm that the pixel will also have the exact volume, the sample is filled with water. The volume is found to be $8,1 \text{ cm}^3$. However, the maximum volume fill by stainless steel powder is around 4.5 cm^3 which is roughly 54% volume fill of the simulation.

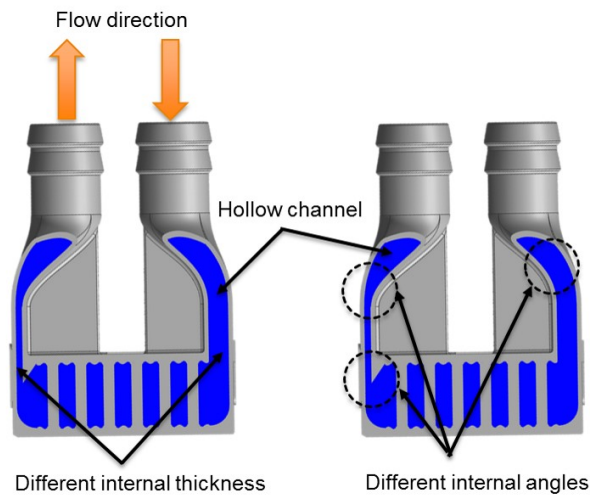


Figure 4: Section view of Aluminum Pixel (AlSi10Mg) with internal features.

Last but not the least, the sample itself has complex shape and internal thin walls at an angle. These regions are marked by dash circle in the Figure 4. The simulation calculated the results based on a fully filled Aluminum pixel where it could be seen that the sample can be completely depowdered under orientations. The experiments are then conducted to validate if the same phenomenon is reproducible in real-life scenario. The summary of the occupancy of the volume fill in sample is given in Table 1.

Table 1: Summary of occupancy of the sample volume

Sample fill in:	Volume(cm^3)
Simulation	8,3
Water	8,1
Powder	4,5

Experimental Setup

A simple experiment is devised where a metal sample (AlSi10Mg) is rotated at around a fixed axis at different orientations in both Counterclockwise Direction (CCW) and Clockwise Direction (CW). The experimental setup can be seen in Figure 5. The plane of reference is provided for ease of interpretation of angle orientations. The arrows in the Figure represent orientation direction, CCW and CW respectively.

Prior to experiments, it was expected that the Aluminum pixel sample will have 100% fill, which would ideally give an indication on how much a sample can be depowdered under the respective orientations. While performing the experiment, it is impossible to fully fill the sample with the powder. Regardless of "shaking" and "tapping" the sample to maximize settling of powder within

the sample, sample with 100% volume fill is not achievable.

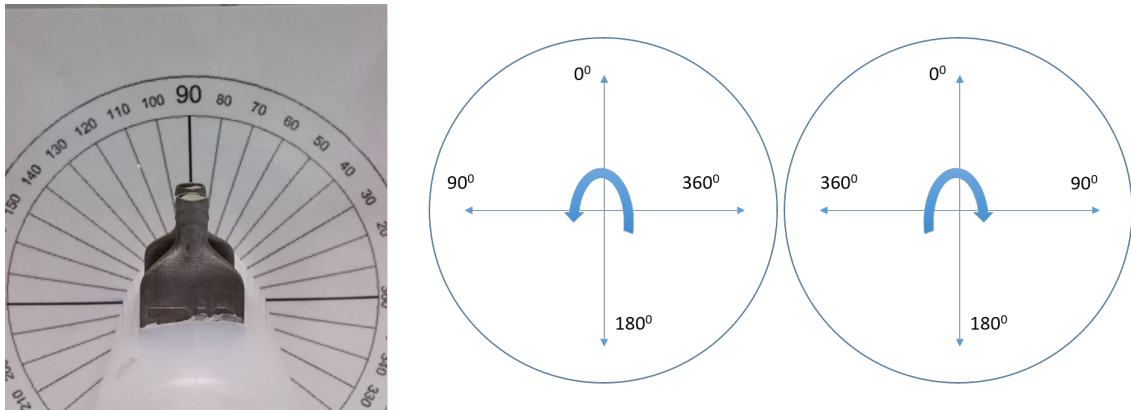


Figure 5: *From Left to right:* Experiment setup with Aluminum Pixel (AlSi10Mg), CCW direction reference and CW direction reference.

The Aluminum pixel is initially weighed in Mettler Toledo scale. After filling the sample with stainless steel powder, it is reweighed. The difference between the weights gives us the amount of powder that has been filled within the sample. It is then carefully mounted on a lab-made setup against a protractor³, as can be seen in the Figure 5. It is manually rotated from 0° to 360° with 10° intervals, first in the CCW direction, and then the experiment is repeated for CW direction. The powder that flows out at every interval of the Aluminum pixel orientation is collected in a circular aluminum lab pan placed in the bottom of the setup. At each interval, the Aluminum lab pan is weighed. The difference between each successive interval provides indication on how much powder flows out at the respective angle orientation. It is noted that CCW direction loses powder differently than in CW direction.

Simulation

In the simulation being developed by Maurice Limpens, the .STL file of Aluminum pixel is sliced in cubic voxel of $250\mu\text{m} \times 250\mu\text{m} \times 250\mu\text{m}$. The Aluminum pixel is then orientated at 10° intervals, first in the CCW direction and then it is repeated for CW direction. The simulation checks if the powder can flow out under respective orientations, and can only flow when there is next empty voxel available for the powder to occupy the voxel space. In the simulation, the Aluminum pixel has 100% powder fill. In the simulation the powder flow is assumed to be ideal where the effects of friction, interlocking and free flow of powder flow are not considered. The roughness of the wall of the sample is also different in the simulation compared to the 3D printed sample.

³90° in the Figure5 represent 0°.

3.2 Results

The results from the experiment are interesting. Although the Aluminum pixel sample does not completely empty, it still emptied 18% and 23% of the total powder-in (53%) in the CW direction and in the CCW direction respectively. This was observed when the sample is *only* rotated and no external excitation is applied. An experiment was also done where tapping⁴ is applied on the sample during the experiment. The depowdering is promoted by tapping. The percentage of stainless steel powder remaining within the sample at each angle interval is tabulated and graphed in Table 2 and Figure 6 respectively.

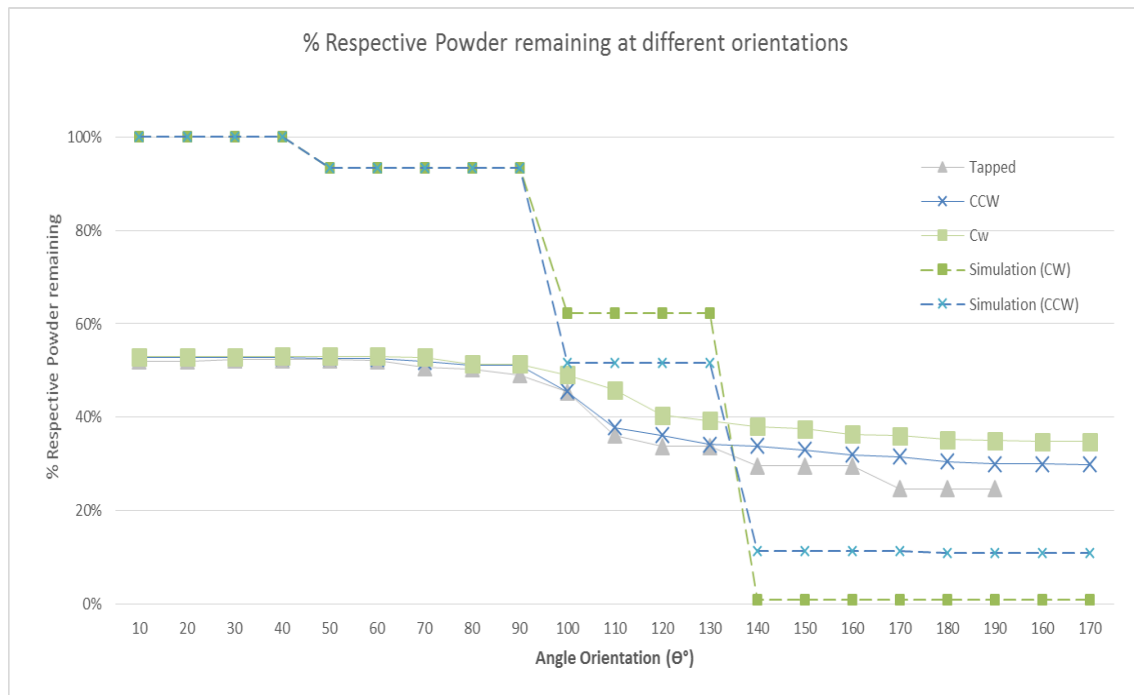


Figure 6: Percentage powder removed over the angle orientation.

In Figure 6, "Tapped" refers to gentle striking of the sample, CCW and CW refers to Counterclockwise direction and Clockwise direction, respectively. The experimental results are represented by solid lines whereas the simulated results are represented by dashed lines. The Aluminum pixel sample could only be filled upto 53% (for CCW and CW) and 52% (tapped) compared to 100% in the simulation.

The most percentage of powder that flows out of the sample is observed between $\theta = 120^{\circ}$ and $\theta = 140^{\circ}$ where 9%, 10% and 13% of accumulative powder in that angle range flows out in the CW, CCW and tapped experiment respectively.

The difference between the percentage of powder flow in CCW and CW direction can be explained due to the internal geometry of the sample. Powder will accumulate in the marked regions in the

⁴Tapping refers to gentle strike on the sample till the point where no powder flowed out the sample at the respective angle.

Figure 7. During the experiments, it was seen that the powder flows out from the above channel compared to the bottom channel regardless of CCW or CW direction. Upon visual inspection, accumulated powder (rathole formation) could be seen in the bottom channel which could be the reason of flow resistance. It is interesting to note that the sample does not loose powder as much compared to other angle orientations when it is at $\theta = 180^\circ$, since one would expect the most depowdering to occur at this angle. At the corresponding angle $\theta = 180^\circ$, the powder accumulates in the flat plate (box in Figure 8) and thus resists flow. This is also true for the simulated results at this angle. The effect of tapping was also checked to see how the powder flow out is influenced. It was observed that tapping promotes depowdering because tapping reduces the resistance of powder flow.

The difference between the experimental and simulated results is that simulation considers the ideal flow behavior of the powder. The friction forces between the powder and the wall are neglected which explains the continuous flow compared to discrete flow in the simulation. Interlocking of powder is observed in the experiments which is not considered in the simulation. The validation was not successful since the experimental model only allowed 54% of the powder fill compared to the simulated results (100% powder fill). Furthermore, the roughness in the simulation is "virtual" and thus the effects of roughness are prominent in the experiment.

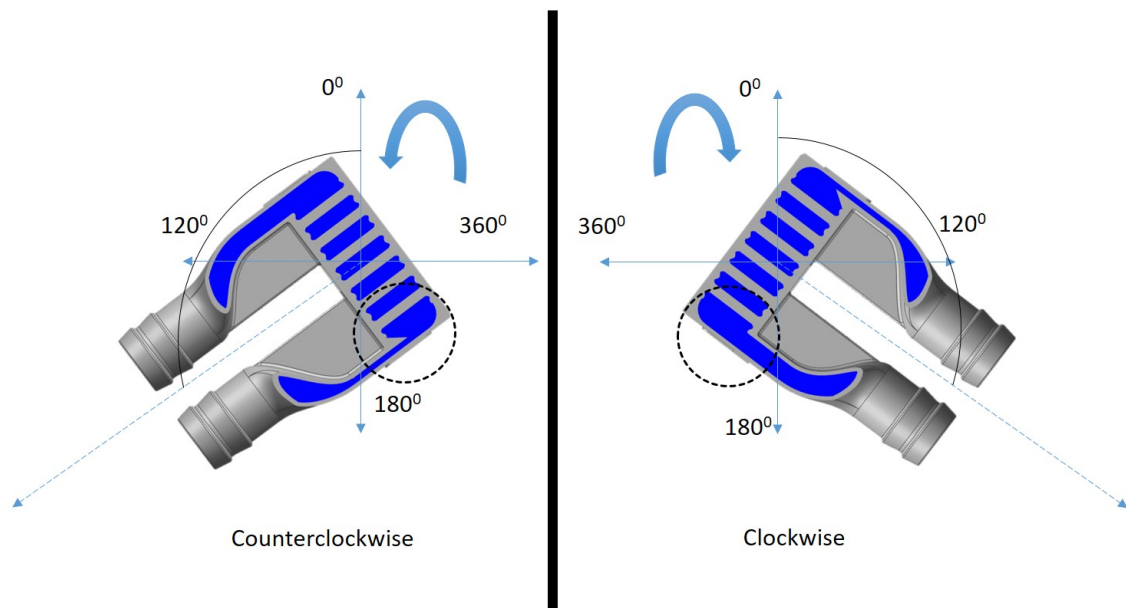


Figure 7: Depiction of Aluminum pixel at 120° .

3.3 Conclusion

The main purpose of the experiments were to validate the simulated results and to confirm if a sample could be completely depowdered. As can be seen from the Results section (3.2), the experiments did not successfully depowder the sample, whereas in the simulation the sample has

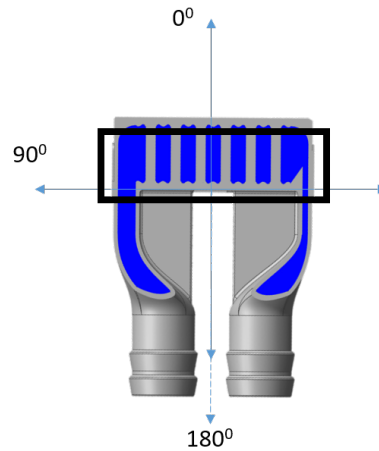


Figure 8: Depiction of Aluminum pixel at 180°.

Table 2: Summary of the powder flow via respective methods

Method	%Powder Fill	%Powder remaining	%Depowdered
Tapped	52%	25%	27%
CCW	53%	30%	23%
CW	53%	35%	18%
Simulation CW	100%	1%	99%
Simulation CCW	100%	11%	89%

almost depowdered. The main aim to completely depowder the sample has not been achieved via this method. The reasons have been stated in the Results section (3.2).

Since the simulation model is still under development, additional parameters such as interlocking, friction forces and roughness of the sample under investigation could be implemented to simulate real-flow behaviour of the powder. As observed by results of tapping in the experiment, the effects of excitation could also be incorporated in the simulation model. The current sample under investigation has not been freshly printed. This meant the sample under investigation was almost powder free to certain extent and required re-filling. Due to the complex geometry of the sample, it could not be filled with 100% powder. Thus, fresh 3D printed samples that have not been post-processed should be tested to see the effects of powder flow under different orientations. Moreover, samples with more complexity, different shapes and sizes should be experimented with and simultaneously compared with simulation model. Mechanical properties of the current powders being used in SLM could also be implemented.

The experiment for powder flow has been lab-made and is thus not an ideal way to experiment. During the experiment, there is friction when rotating the setup which also provides misleading indication of how much the actual powder flows out. It was best made sure to have as smooth of a rotation to have minimal impact on powder flow from the effect of friction. The experiment setup

can be greatly improved by using better fixtures and using frictionless rotational mechanism, such as bearings.

Having said this, the main goal of this internship had not been achieved until this point, i.e. complete depowdering of the 3D printed sample. Thus, available potential cleaning techniques will now be explored to find and deduce the ideal method for cleaning the sample.

4 Cleaning Techniques

Of all the possible ways to depowder or clean a sample, few cleaning techniques (namely Laser shockwave cleaning (LSC), Ultrasounds, vibrations) are going to be explored. These techniques have been studied in depth and relevant literature is available explaining the underlying principles and dynamics of particle removal. A brief description on such techniques that have been explored for depowdering during the course of this internship are provided in this part of the chapter, along with an additional possible cleaning technique that could be used but is limited in terms of available knowledge (Electromagnetism).

While there are many possibilities to depowder or clean a sample, not all the techniques were studied in depth during the course of internship. Instead, the technique which has the most potential and has shown evidence of cleaning will be prioritized. The main decision factors for choosing the relevant cleaning techniques were the particle size to be removed, availability of cleaning equipment, and has shown previous potential for cleaning for the respective particles under study.

An industry specializing in SLM production need to guarantee the final product is internally empty and clean. Certain industries such as electronic industries are constantly looking for efficient ways to remove small particles (typically in the range of nanometers) from their products, for e.g., Si wafers. Minute particles of dust or other contaminants could affect the performance of the chip (Dunbar *et al.* (2007), Lammers *et al.* (2008)). Conventional cleaning techniques such as wet cleaning, chemical cleaning, megasonics and CO₂ cleaning are unable to meet the current cleaning regulations and requirements of microindustries as they advance and produce much smaller (submicron and nanometers(Dunbar *et al.* (2007)) structures and samples.

Not enough data or information is present on the removal of particle from the surface of 3D printed structures. As this internship primarily focuses on depowdering of metal structures produced by SLM, previous principles and data on particle removal for thin plates will be taken as a guideline to understand the particle removal behavior as under microscopic level. The particles can be viewed as attached to a thin metal plate. The following techniques for particle removal are:

- Laser Shockwave Cleaning (LSC)
- Electromagnetism
- Chemical Flushing
- Vibrations and gravity
- Ultrasounds

Each of the cleaning techniques is discussed in the following section.

4.1 Depowdering Techniques

4.1.1 Laser Shockwave Cleaning

One of the techniques for particle removal is via shockwaves produced by Lasers. The particles are removed through a fast moving shockwave, which is generated via laser induced breakdown (LIB) of air. This happens when air is exposed to very intense electromagnetic wave, where the light of high energy pulse is focused in a very small volume. The Figure 9 shows the schematic drawing of particle removal by laser breakdown.

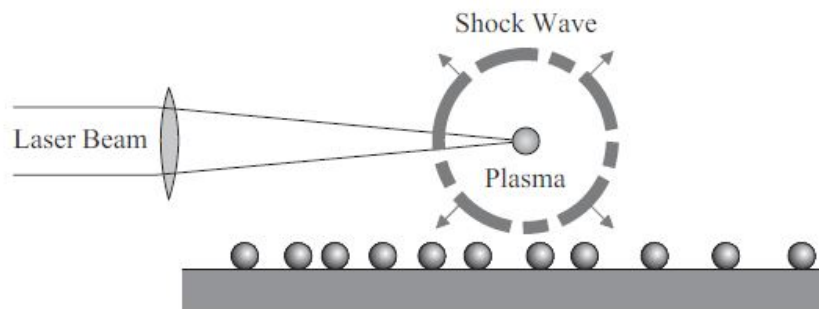


Figure 9: "Laser Shockwave Cleaning (LSC). The focused laser pulse creates small plasma above the contaminated surface. The plasma expands at such a high rate that it generates a shockwave. The shockwave is used to remove the particles from the contaminated surface." (Source: Master Thesis, Laser Shockwave cleaning, Technical University Eindhoven Lammers *et al.* (2008)).

Before each cleaning process, plasma is created every time at the focal point of the lens. This plasma results from air being ionized when the intense electromagnetic field of the laser starts the laser Induced Breakdown (LIB) of air. The LIB during the LSC process generates a highly pressurized air bubble which expands at supersonic velocity. A shock front is created which "sweeps" away the air in its wake. A spherically expanding shockwave is created by LIB by focusing the laser pulse at the focal point of convex lens. Given the nature of high pressurized air bubble that is created during the process, there could be thermo-mechanical damage risk and heat radiation effects on the structure. However, this is minimized by using appropriate height above the surface at which the LIB is created, also known as the gap distance. Dunbar *et al.* (2007)

It should be mentioned that LSC has been performed on Si-wafers, more precisely on thin flat plates with particles in the submicron and/or nanosized particles. There is limited experimental data available on micron-sized particles. The process is limited by the fact that LIB cannot be produced at low laser pulse energies. The LSC process has been done for Extreme Ultraviolet (EUV) lithography where the particles to be removed are in nanometer range.

As the focus of particle removal is in the micrometer range, doing such an experiment just to investigate the effects on micron-sized particles is unnecessary, expensive and requires extensive time to set up the experiment. Also, since shockwaves are created via LIB of air, creating plasma

within the structure is out of the question as this can do serious damage to the structure. At this stage, it is not also possible to control the position of the plasma. The propagating waves generally lose energy as they travel over the distance, and thus focusing particles in dead zones or long channels will be a challenge.

4.2 Electromagnetism

As of yet, there exists no data on cleaning by electromagnetism. Electromagnetism allows the possibility for creating an electromagnetic field and forces such that magnetic levitation can occur. Levitation could be one of the methods for transporting loose particles out of the geometry. Unfortunately, no simulation or experimental data is available to defend the cleaning effectiveness of this method. A simple model, however, could be constructed for a particle resting in electromagnetic field. Since these forces are either repulsive or attractive in nature, these forces could be manipulated such that they could transport loose particles in the electromagnetic field, either via levitation or external flowing fluid through the structure. Magnetic levitation already exists and forces in play are well understood.

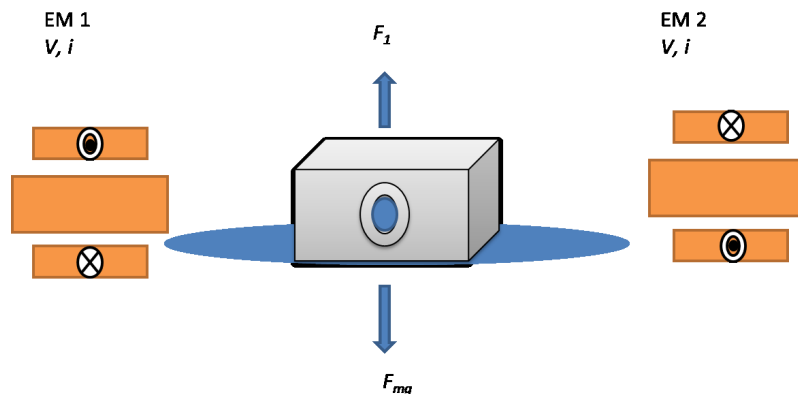


Figure 10: Schematic representation of metal subjected to Lorentz, electromagnetic induction to levitate the object.

To visualize the setup, the schematics can be seen in Figure 10 and 11. Basically, a magnetic levitation system such as depicted in Figure 10 having electromagnets will generate Lorentz forces. In the Figure 11, the entire region between the magnets has electromagnetic fields, however, to create an impression of how the electrical and magnetic forces act on the particle are shown under colored regions where red expresses the electrical force whereas the blue region denotes the magnetic field.

Microscopically, the particles have electrostatic and electrical double layer as two adhesion forces. Primarily, these forces would need to be overcome for modeling particle removal behavior. Due to lack of knowledge on this matter, there is no experimental data on the efficiency of the cleaning technique, or if it is feasible in the first place. To get insight on this topic expertise of Dr. Ir. Martijn van Beurden (Associate professor in Electromagnetism at Eindhoven University of Technology)

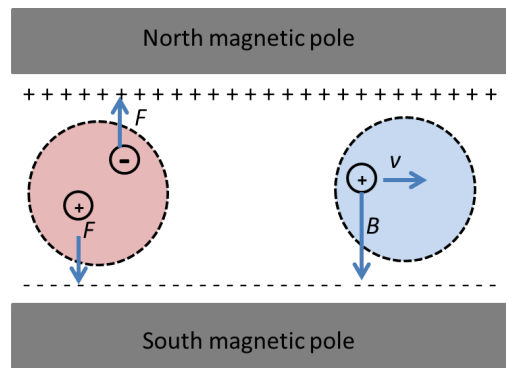


Figure 11: Schematic representation of individual particles subjected to electromagnetic field. For ease of visualization, red denotes electric field, whereas blue denotes the magnetic field. It should be noted that the entire region within the magnets is under electromagnetic field.

was taken into consideration.

According to Dr. van Beurden, extensive experiment set up (Electromagnetic setup) is required to perform cleaning experiments. Since the sample structure and the powder are of the same material, the structure and powder will have the same electrical charge and magnetic polarities under the electrical field and magnetic field respectively due to electromagnetic induction. Thus manipulating such forces for reverse polarity or having a force at a specific point within the sample structure is a challenge at the moment. Also, due to inverse square law, the energy density of the wave decreases inversely as the square of the distance from the source. Furthermore, the electromagnetic field will have equal strength over the entire global region.

4.3 Chemical flushing

This technique makes use of chemical agents rather than an external equipment, as compared to the cleaning techniques mentioned above. Instead of creating external forces (shockwaves or levitation), chemical agents that are widely used in industry for flushing purposes could be applicable for the cleaning study. Since broad materials (metal, plastics, ceramics etc.) can be now be printed by 3D printing, not all the materials would be suitable for cleaning with chemicals, as they may either react violently or become victim to corrosion.

Extensive research would be required and there is no guarantee that the structure would remove the powder. If the structure with an empty structure is densely packed with powder, the cleaning agent may not be able to penetrate through these channels and might get deposited itself. Furthermore, quick test with water flushing through the 3D printed structure shows that the 3D printed metals absorb water to certain extent. This could mean the same phenomenon could happen for such chemicals. A chemical agent could be made such that it is non-corrosive, has relatively low boiling point similar to Acetone such that it will not accumulate inside the channel (simple heating of structure would evaporate the chemical) and has low viscosity (compared to water). Due to low viscosity, the chemical should be able to flow out at orientations where gravi-

tational forces are in favor. The advantage compared to other techniques presented so far is that it does not require large external setup. This technique could be investigated, however, majority of the cleaning chemicals pose an environmental hazard and extreme caution needs to be taken during the cleaning process. There is no such "one" chemical agent that could be used for all materials. To gather this information would mean long hours of experimentations and determining the types of chemicals specific for specific materials would require extensive trial and error. This is not possible during the course of internship, and thus this technique will not be considered at this time of study.

4.4 Vibrations and gravity

External vibrations enforced on the structure could also lead to detachment of particles from the vibrating surface. The vibrating surface should be oriented such that the gravitational forces promote the powder removal. Similar technique to remove a particle from the surface has been discussed in Chapter 3, however this technique additionally uses external vibrations for particle removal. The effects of "tapping" already shows promise for promoting particle removal.

Particle removal thus could also be done through vibration. Orientation of the structure plays a crucial role at which maximum powder is removed from the structure. This is also what is found during the experiments and simulations.

While vibrations and gravity do remove particles, the results were not successful at this point. Extensive testing and experimentation for removal of particles via vibrations would be required for the respective samples under study. Also, prior knowledge of materials properties is required to know the natural frequency of each and every sample structure. This requires extensive research. Regardless, a small experiment was done to validate the Gravity and vibration Model Simulation.

4.5 Ultrasonic Cleaning

Ultrasonic cleaning is extensively used for industrial cleaning applications. Ultrasonic waves are produced through transducers when an electrical field is applied to piezoelectric crystals. The crystals vibrate and produce sound waves as a result of mechanical distortion caused by the electric field. Frequencies between 20 kHz and 1 THz can be produced depending on the application of the ultrasounds. For cleaning applications, the ultrasound frequencies lie between 20 kHz - 40 kHz.

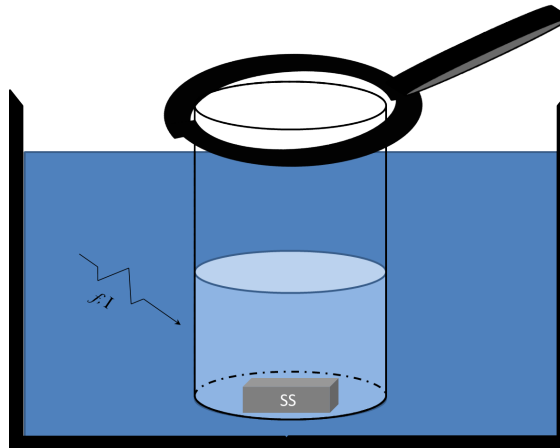


Figure 12: Schematic representation of metal submerged in water in a beaker held by a clamp.

Figure 12 represents the schematic view of ultrasound cleaning. The ultrasonic cleaning technique for particle removal depends on mechanisms of acoustic cavitation and chemical solvation. Cavitation forces can have undesirable effects on the structure being cleaned, and are generally hard to control whereas solvents are environmentally hazardous. According to Qi & Brereton, water is a great solvent and can be applied where low cavitation thresholds are desired. The cleaning force is the shock waves produced by micro-cavity. These cavities or vacuum bubbles range from 50 to 150 μ m. As mentioned before, the particles of our interest are well under this range, furthermore the Ultrasound bath available for testing operates at ideal frequency range ($f=40$ kHz) for particle removal Visser (1995, Table 5.1).

The cleaning parameters are primarily dependent on cavitation intensity. Cavitation depends on the frequency and amplitude of the radiating wave. It also depends on the mechanical properties of the acoustic medium, and the rheological properties of the liquid under turbulent and laminar flow.

When the structure is submerged under water and exposed to ultrasounds, the particles suspended in the liquid oscillate and experience acceleration. What makes ultrasonic cleaning attractive is the ability to remove particles out of small pores and crevices (Visser, 1995, page 221). Thus, Ultrasounds look like the prime method for depowdering. In spite of being the favorable choice for cleaning, other methods are still considered before making a final decision on the mode of cleaning.

4.6 Final selection of cleaning technique

The main focus of this report is to find the efficiency of the method chosen for depowdering. A table with the benefits, limitations, risks and possible effects on structure have been tabulated below 14. As can be seen in the table, the final decision was made on the basis of feasibility, availability and practicality of the cleaning technique. Table 13 was tabulated for the decision

making. As is summarized in the decision table, the main factor that influenced the decision for cleaning technique was the size of particles to be cleaned. Of all the techniques mentioned in the table, Ultrasound and the respective equipment are readily available at TNO for testing, whereas the rest of the cleaning techniques require additional times on making the setup. Since the particles in micron-sized range are investigated, time limitations and requirement for high degree of cleanliness of complex structures with internal channels. As a result ultrasonic cleaning is the selected choice for cleaning.

Decision factors for cleaning	Cleaning techniques	Ideal for:	Final Choice
1) Particle size: Microparticles	Laser Shockwave →	Nano-sized- particles	Ultrasounds
2) Equipment readily available (@ TNO): Ultrasounds , vibration, chemical flushing	Ultrasounds →	Microparticles	
3) Time duration of internship.	Gravity/Vibration	Micro-nanoparticles (limited info.)	
4) Least hazard and least expertise to operate.	Chemical flushing		
	Electromagnetism		

Figure 13: Decision parameters that led to selection of ultrasound

Method	Benefits	Limitations	Risk	Effect on the structure	Extra Equipment Required
Vibrations and gravity	<ul style="list-style-type: none"> - Least expertise required - Particle removal by excitation - Not much equipment needed - Ease of use - Vibration will detach particles 	<ul style="list-style-type: none"> - No view on dead spaces, require visual and internal inspection - Need to know the ideal orientation - Need to know natural frequencies of all available material 	<ul style="list-style-type: none"> -If vibrations = resonance frequency, structure will be heavily affected 	<ul style="list-style-type: none"> - Structural damage and mechanical failure if $f_{\text{natural}} = f_{\text{resonance}}$ 	<ul style="list-style-type: none"> - Frequency generator
Laser shockwaves	<ul style="list-style-type: none"> - Improved properties of dense material - No thermal stresses induced - Energy density could be varied to target different sized particles 	<ul style="list-style-type: none"> - Longer cleaning process (2 - 3 runs) - Waves may not propagate into the tubes - Skilled operator - Small gap distance (LIP and substrate) could induce thermo-mechanical effects (d<1mm) - Selection of wavelength - Focuses removal of particles 100 – 200 nm 	<ul style="list-style-type: none"> - Overheating, structure damage, internal damage - Laser Irradiation 	<ul style="list-style-type: none"> - Microstructure: Extensive plastic deformation @ $P_{\text{shockwave}} \gg \text{Yield strength}$ - Hardness: Increased Hardness on the surface - Tensile Strength: Increased - Residual Stresses: Compressive yet uniform throughout the radius of laser shocked region - Fatigue: Significantly improved life-cycle 	<ul style="list-style-type: none"> - Q-Switched Nd:YAG laser - Argon gas - Protection gear
(Electro)Magnetism	<ul style="list-style-type: none"> - Individual or cluster of powder could be controlled at the same time 	<ul style="list-style-type: none"> - Creating Maglev may be challenge - No previous knowledge 	<ul style="list-style-type: none"> - Entire structure and powder being equally electromagnetically induced - Powder stuck in deadzones will be stuck to the internal wall 	<ul style="list-style-type: none"> - Entire structure being magnetised. - Increased adhesion 	<ul style="list-style-type: none"> - Electromagnets - AC coils
Ultrasonic	<ul style="list-style-type: none"> - Ideal for micron sized particles - Different frequencies target different particle sizes - Demi water enhances particle removal (Environment friendly) 	<ul style="list-style-type: none"> - Reflection from acoustically “hard”, - Can remove micron sized particles (0,1, 1, 10 micron) - Long cleaning times 	<ul style="list-style-type: none"> - Selection of solvent for respective material - Chemical reaction between solvent and material 	<ul style="list-style-type: none"> - Wrong intensities could damage the structure (more cavitation) 	<ul style="list-style-type: none"> - Ultrasound set-up
Chemical flush	<ul style="list-style-type: none"> - Non-corrosive - Low Boiling point 	<ul style="list-style-type: none"> - Evaporates at RTP - Toxic 	<ul style="list-style-type: none"> - Contamination - Health risks - Flammable - Proper ventilation needed 	<ul style="list-style-type: none"> - Possible contamination and corrosion 	<ul style="list-style-type: none"> - Acetone solution

Figure 14: Summary of all discussed cleaning techniques with pros and cons.

5 Ultrasonic cleaning

As can be seen in Figure 15 ultrasounds have different applications specific to different frequencies. The required frequency range for ultrasonic cleaning application is 20-40 kHz. Such an ultrasonic bath is available within TNO. In addition, there were already 3D printed samples that vary from simple geometries to complex geometries. Ultrasonic cleaning is then performed on these samples.

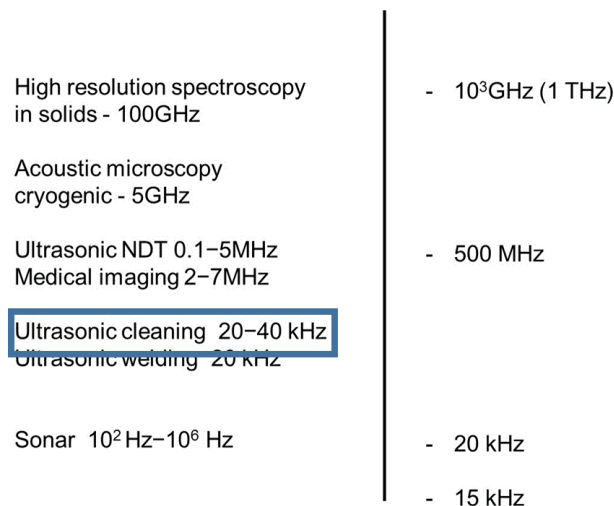


Figure 15: Acoustic frequency scale and selected applications

During ultrasonic cleaning, the most important phenomenon for particle removal is cavitation. As the ultrasonic waves propagate through the water medium in the bath, compression and rarefaction of the medium molecules occurs. This results in implosion of cavitation bubbles. The collapsing micro-bubbles could reach high localized temperatures and pressures ((Mittal & Jaiswal, 2015, page 207)) which are able to produce high shear energy waves and turbulence in the cavitation zone. Also, the cavitation bubble size is inversely proportional to the frequency.

The apparatus was placed under a lab fume hood due to safety regulations. The airflow inside the fume hood is faster than the outside room. Under faster airflow, the rate of evaporation of water increases compared to natural airflow in the room. During long operation of ultrasound (more than 2 hours) the temperature of the water in the ultrasound bath can reach high temperatures. Higher temperatures also promotes the rate of evaporation and thus the water in the bath decreases. If the amount of water in the bath is lower than the recommended level fill, the cleaning performance will be reduced. Therefore, more water had to be added to the bath every hour to ensure the water remains at the optimum level during operations.

During cleaning experiments, each respective sample is placed in a demineralized water solution in a glass beaker. This beaker is later submerged in the ultrasound bath. Without the beaker the metal samples placed directly in the bath can cause severe damage to the tank. Moreover, the removed particles during the cleaning process will foul the bath. However, the ultrasound waves

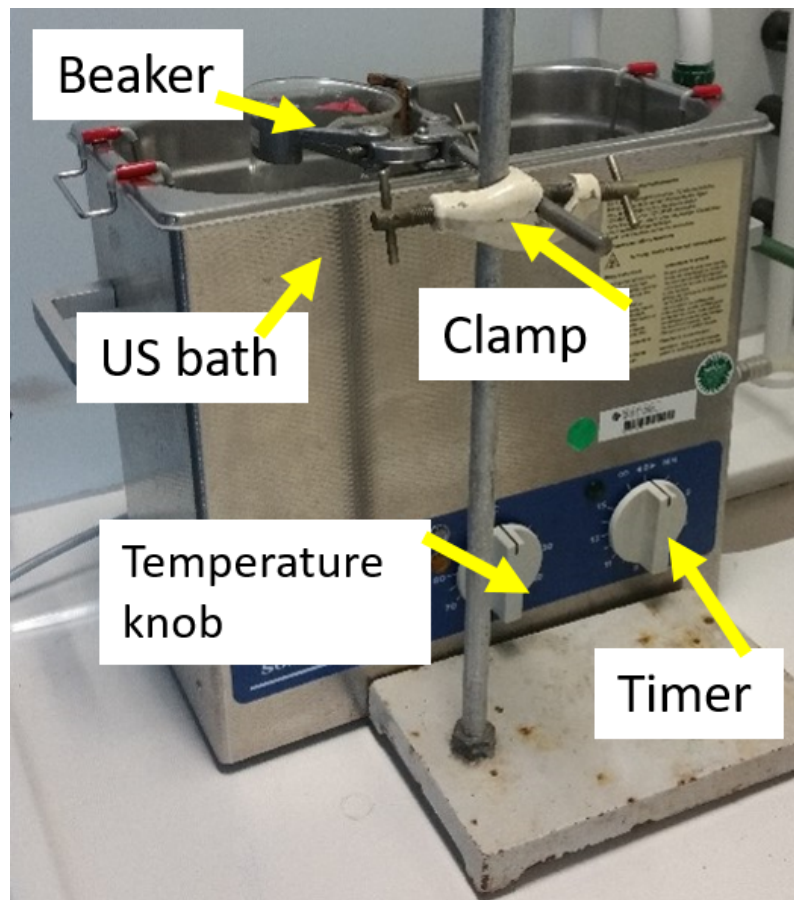


Figure 16: Bransonic Ultrasound bath

can pass through the glass beaker without losing its energy and is thus used to prevent damage and fouling of the water bath and tank.

To account for the limitation of functionality of the equipment during required long hours of cleaning (beyond office hours), the experiment was modified where two water bottles are added upside down to the setup. The bottle accounts for any evaporation losses occurring in the bath and the glass beaker respectively, during the operation by simultaneously maintaining the water at minimum operating level at all times. The set up can be seen in Figure 17.

5.1 Ultrasonic cleaning of the samples

Ideally, freshly 3D printed samples should be used for checking the level of cleanliness achievable from the ultrasound waves. TNO does not produce or manufacture 3D printed metal samples. Rather the metal material parts and samples are delivered by external manufacturer specializing in 3D printing, namely NLR⁵ and ASML⁶. Requesting new single customized complex samples

⁵Nederlands Lucht- en Ruimtevaartcentrum (NLR) is Dutch aerospace industry involved in SLM

⁶ASML Holdings, a Dutch company and world's largest supplier of photolithography systems

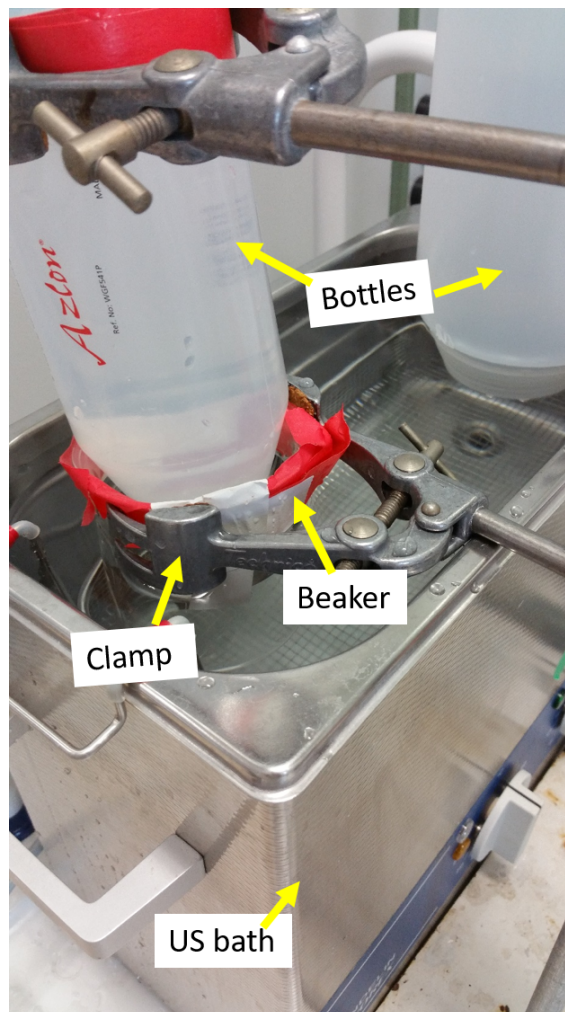


Figure 17: Ultrasonic cleaning setup for 24 hours with 1 bottle for beaker and 1 bottle for bath

from NLR is too expensive unless ordered in batches. Moreover it would take roughly about a month to receive a sample. Thus, the available printed samples will be used for testing. The samples have been previously cleaned via compressed air or chemical flushing.

A total of six different 3D printed metal samples available within TNO were used for cleaning experiments. In the beginning, the cleaning experiment was first done on a stainless steel cooling jacket (Figure 18). As the internship progressed, new samples became available and were received one after another. The second cleaning experiment was done on an aluminum alloy (AlSi10Mg) pixel (Figure 19), followed by ultrasonic cleaning of a stainless steel pipe fitting (Figure 20), concluded by cleaning of 2 stainless steel plates (designated A15 and A16 for ease of identification)(Figure 21). Three separate conventionally mass manufactured stainless steel samples which are Hex nut (Figure 22), Metal plate (Figure 23) and Bolt nut (Figure 24) were also tested to compare the effects on the sample due to ultrasonic waves exposure.



Figure 18: Stainless steel cooling jacket



Figure 19: Aluminum alloy pixel AISi10Mg



Figure 20: Stainless steel pipe fitting

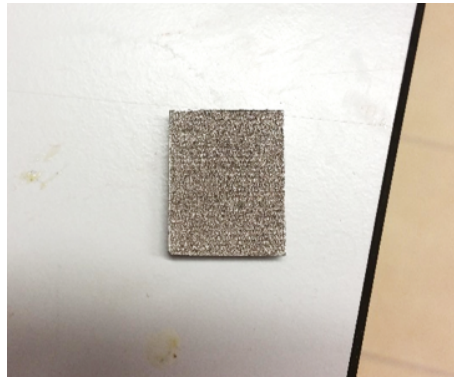


Figure 21: Stainless steel plate A15



Figure 22: Conventional hex nut



Figure 23: Conventional stainless steel metal plate



Figure 24: Conventional stainless steel bolt nut

5.2 Experimental Procedure

Before doing the cleaning experiment, the samples were placed in preheated oven at 150°C for a minimum of ten minutes. The temperature of the oven is selected to reach an ideal environment that will ensure there is no moisture content within the test samples under the given time frame. Since the changes in weight will give an indication on the amount of powder removed(cleaned) from the samples under ultrasound cleaning, the samples were weighed to know the initial weight (W_o).

When the first series of experiments were done, only the stainless steel cooling jacket sample was available for immediate testing. Naturally, the first cleaning experiment was done on the stainless steel cooling jacket sample. For this sample only, stainless steel powder (readily available within TNO) is first filled in to the sample. Prime reason for filling the sample with powder is to emulate a freshly printed filled sample. The sample is reweighed (W_{sp}) and the amount of powder (W_{powder}) that is present within the sample is now known. The weight of the powder inside the sample is calculated by Equation 5.1

$$W_{powder} = W_{sp} - W_o \quad (5.1)$$

where W_{powder} is the weight of stainless steel powder in the sample, W_{sp} is the weight of the sample with powder and W_o is the initial weight of the sample without powder.

The sample is then placed in the glass beaker submerged in the ultrasound bath for different time duration and the cleaning experiments can begin. The sample is reweighed after each cleaning cycle; the drop in weight indicates how much powder has been removed after each cleaning cycle. The sample was also visually inspected for damages after every cleaning cycle.

As the cleaning experiments on the cooling jacket sample progressed, the results from initial cleaning of the stainless cooling jacket sample were not promising. After few consecutive series of cleaning experiment on the sample, the weight of the cooling jacket surpassed its initial weight (W_o). The sample continued to show indefinite weight loss. The time to cleaning hours could not be determined. Unfortunately the results are unreliable and cannot provide a good indication of cleaning via ultrasounds. Thus, a series of cleaning tests were then performed on conventional mass produced stainless steel samples to see whether the same phenomena is observed. These samples did not lose any weight under ultrasound cleaning and thus it was concluded that the cooling jacket sample is faulty. To confirm this theory, the stainless steel cooling jacket was tested under microscope where large voids are seen in the surface of the sample. The other 3D printed samples (Aluminum pixel, stainless steel pipe fitting and steel plates [A15, A16]) were then received in the order stated.

It was brought to attention that Al pixel and ASML pipe fitting have been previously cleaned via air and/or chemical flushing. To test whether these samples were in fact clean, no additional powder was added to these samples. Due to the consequence of poor results from the stainless steel cooling jacket, the samples A15 and A16 were received as a replacement. Since these samples

are simple solid metal plates, stainless steel powder was not used for filling the sample.

The latter samples performed well under the cleaning experiments. The samples (apart from stainless steel cooling jacket) did reach a limit to which they could be depowdered. The cleaning limit was reached when there was no subsequent weight drop of samples from its predecessor weight. To confirm the limit, a final cleaning experiment is done for each sample where the final weights of the sample after cleaning experiments are compared to its former weight just before the final instant of cleaning experiment. No net difference in weights concludes the experiment and thus the limit to which a sample can be cleaned. The results of each respective sample are presented in the following section of the report.

5.3 Results from ultrasonic cleaning

The cleaning results through the use of ultrasounds did in fact show promising results. These are tabulated below for each respective sample. The observations made during the cleaning experiments are also discussed briefly.

5.3.1 Stainless steel cooling jackets

The first cleaning experiment was performed on the stainless steel cooling jacket sample. The initial weight of the sample before the experiment is $W_o = 80,6773g$. Stainless steel powder (LPW316L) was used to fill the sample, where the $W_{sp} = 80,8424g$. As can be seen from Table 3, the first column shows the number of cleaning cycles required to depowder, the second and the third column represent the subsequent weight changes as a result of cleaning under certain duration. The difference of the weight is calculated to know how much powder is removed from a sample at each instance of cleaning. At cleaning cycle C_2 , the weight of the sample was found to be lower than initial weight ($80,6599g < 80,6773g$).

During the cleaning experiment, it was noted that the stainless steel cooling jacket samples continued to show weight loss after prolonged cleaning. There are two speculations for weight loss: 1) There is still powder inside the sample, 2) Corrosion. Due to the geometry of the sample, the first assumption could be over-ruled since there are no dead spaces present within the sample. The sample can be seen with inter-connecting simple straight inlet and outlet holes, depicted in Figure 25. As can be seen, the sample has no complex internal chambers or dead spaces. To confirm the latter speculation, conventionally produced stainless steel pieces were experimented with ultrasounds. With the cleaning experiment, it could be concluded that there is no weight loss by corrosion. To understand the reason for weight drop, the sample has been then inspected via microscope to check the sample properties of the structure. It was found that the sample had poor density packing and consisted of large voids and cracks. It was also discovered that the sample had been printed at the stage where little was known about SLM in terms of structure integrity.

After the cleaning tests on conventional samples, corrosion can be safely neglected. These can

Table 3: Ultrasonic cleaning of stainless steel cooling Jacket

Clean Cycle (C)	Initial weight(g)	Weight After cleaning (g)	Duration	Difference (g)
0	80,8424	N/A	N/A	0
C ₀	80,8424	80,6979	10 minutes	0,1445
C ₁	80,6979	80,6886	15 minutes	0,0093
C ₂	80,6886	80,6599	30 minutes	0,0287
C ₃	80,6599	80,6531	1 hour	0,0068
C ₄	80,6531	80,6503	1 hour	0,0028
C ₅	80,6503	80,6487	1 hour	0,0016
C ₆	80,6487	80,6457	10 hours	0,0030
C ₇	80,6457	80,6421	30 minutes	0,0036
C ₈	80,6421	80,6403	1.50 hours	0,0018
C ₉	80,6403	80,6341	24 hours	0,0062
C ₁₀	80,6341	80,6196	24 hours	0,0145
			Total Duration	Net Difference
			64 hours	0,2228(g)

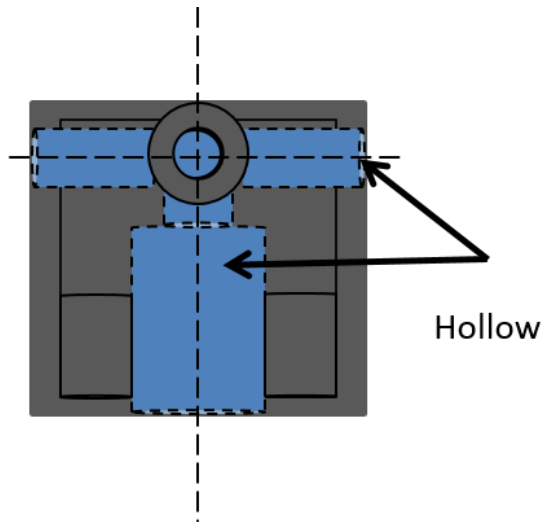


Figure 25: Internal view(Represented by blue color) of the stainless steel cooling jacket

be seen in Table 4 till 6 where no apparent weight loss is observed regardless of varying the temperature or long cleaning durations.

Table 4: Ultrasonic cleaning of conventional stainless steel Hex nut

Clean Cycle (C)	Initial weight (g)	Weight after cleaning (g)	Duration	Difference (g)
C ₀	3,9549	3,9549	15 minutes	0
C ₁	3,9549	3,9549	20 hours	0
			Total Duration 20.25 hours	Net Difference 0 (g)

Table 5: Ultrasonic cleaning of conventional metal stainless steel plate

Clean Cycle (C)	Initial weight (g)	Weight after cleaning (g)	Duration	Difference (g)
C ₀	74,6335	74,6316	2 hours	0,0019
C ₁	74,6316	74,6316	4 hours	0
C ₂	74,6316	74,6316	2 hours	0
			Total Duration 6 hours	Net Difference 0,0042(g)

There seems to be some weight loss in the case of the metal stainless steel plate. This is explained by the fact that there were holes drilled in the metal plate. These have not been deburred to great accuracy, and hence particles were lost as a result. As can be seen from the results, after first cleaning cycle, it does not lose further weight.

Table 6: Ultrasonic cleaning of conventional stainless steel bolt nut

Clean Cycle (C)	Initial weight (g)	Weight after cleaning (g)	Duration	Difference (g)
C ₀	19,552	19,552	15 minutes	0
C ₁	19,552	19,552	4 hours	0
C ₂	19,552	19,552	2 hours	0
			Total Duration 6.25 hours	Net Difference 0,0000(g)

During the cleaning experiments, it could be observed that there were two ways on how the powder that was removed behaved under the water. It should be noted that stainless steel ($\rho_{ss} = 7.99g/cm^3$) has higher density than water ($\rho_{water} = 1g/cm^3$). Regardless, a small amount of powder was seen to float on the surface of the water. This powder is rather "loose" in nature, and some powder (packed) could be seen resting on the bottom of the beaker. This can be explained by surface tension of the water. Packed powder at the bottom has higher packing compared to the floating powder. Higher packing leads to higher density and thus compared to loose powder is heavier and thus is found at the bottom of the beaker. Although it was hard to capture the image,

they have been shown in Figure 26 and 27.

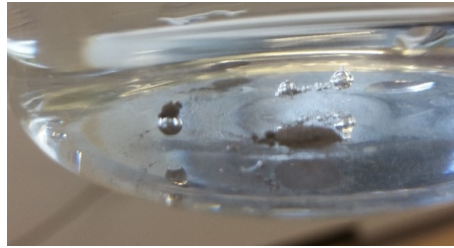


Figure 26: Removed powder over bubble



Figure 27: Powder removed

5.3.2 Aluminum alloy pixel (AlSi10Mg)

The above sample did not give indication of the cleaning efficiency via ultrasounds. Thus, the next sample with better material properties was needed to conclude whether ultrasounds is indeed an effective method for cleaning. For this, the next sample received was the Aluminum pixel. The Aluminum pixel has been designed by TNO but printed at NLR. So far this is one of the most complex sample compared to other samples under study. This pixel has internal fins and has orifices of less than 1 mm in diameter. The section view is given in Figure 28 to show the complexity of the shape.

When the Aluminum pixel was handed, it was mentioned that this sample was previously "cleaned". To confirm this statement, the cleaning experiment was performed on the sample as it was received. Moreover the fact that it has been cleaned before, made it a prime sample for cleaning under ultrasounds since technically it should not lose weight. The initial weight of the sample is $W_o = 26,5959g$. The results of cleaning are tabulated in Table 7.

As can be seen from the Table 7, the sample did lose weight and does have a limit to which it can be cleaned. The sample needed a total of 26,5 hours to be cleaned with four consecutive cleaning

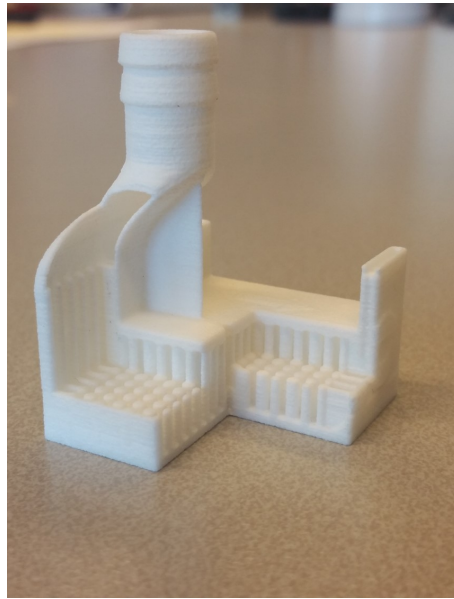


Figure 28: Cross-section view of Aluminum pixel

Table 7: Ultrasonic cleaning of Aluminum pixel (AlSi10Mg)

Clean Cycle (C)	Initial weight (g)	Weight after cleaning (g)	Duration	Difference (g)
C_0	26,5959	26,5487	1 hour	0,0472
C_1	26,5487	26,5481	1.50 hour	0,0006
C_2	26,5481	26,5214	22 hours	0,0267
C_3	26,5214	26,5178	2 hours	0,0036
C_4	26,5178	26,5178	2 hours	0,0000
			Total Duration 28,5 hours	Net Difference 0,0781(g)

cycles. Considering the time required for cleaning, the particles were removed at 2,9 mg/hour for a total of 26,5 hours. The sample is placed for another 2 hours (C_4) as a final test and no further decrease is noticeable. This means that the sample is powder free and should not have internal blockages during its function.

5.3.3 Stainless steel pipe fitting

Obtaining successful result from one sample is not enough. Hence, additional experimentation is required. The next sample received for cleaning experiment was the stainless steel pipe fitting designed by ASML. Just like the previous Aluminum pixel sample, this sample has been previously cleaned by ASML. This sample is also not filled with powder. Accordingly, it shouldn't lose weight and no particles are expected to be removed. The results of the sample is tabulated in Table 8

Table 8: Ultrasonic cleaning of stainless steel pipe fitting

Clean Cycle (C)	Initial weight (g)	Weight after cleaning (g)	Duration	Difference (g)
C ₀	49,8167	49,8153	1 hour	0,0014
C ₁	49,8153	49,8149	1.50 hour	0,0004
C ₂	49,8149	49,8149	2 hour	0,000
C ₃	49,8149	49,8149	5 hour	0,000
			Total Duration 9.5 hours	Net Difference 0,0018(g)

Unexpectedly the sample did lose particles. A total of 1,8 mg of sample particles was found to have been lost from the sample before it comes to limit where no further decrease is seen. The limit point can be observed in third cleaning cycle (C₂). Two additional cleaning cycles of 2 hours and 5 hours each were further conducted to see whether additional particles are lost or not. No net difference in the weight concluded that no further particle removal is possible. The sample lost a total 0.72mg/hour in about 2.5 hours of cleaning. Regardless of being cleaned previously prior to ultrasonic cleaning, the sample still lose weight. These were relatively removed with ease within a total of 2.5 hours. The sample is now clean.

5.3.4 Stainless steel metal plate A15 and A16

Discussing the findings of the Stainless Steel Cooling jacket with the supervisor, two individual 3D printed metal plate samples (designated A15 and A16) were then given and placed under ultrasound baths. The two experiments differ in the operating temperature conditions: A15 was cleaned at ambient conditions whereas A16 is cleaned at 60°C. These metal plate samples have better mechanical properties compared to the stainless steel cooling jacket sample. The results from cleaning A15 are given in Table 9.

Table 9: Ultrasonic cleaning of metal stainless steel A15

Clean Cycle (C)	Initial weight (g)	Weight after cleaning (g)	Duration	Difference (g)
C ₀	17,7546	17,7538	2 hours	0,0008
C ₁	17,7538	17,7527	6 hours	0,0011
C ₂	17,7527	17,7520	6 hours	0,0007
C ₃	17,7520	17,7512	7,5 hours	0,0008
C ₄	17,7512	17,7509	7 hours	0,0003
C ₅	17,7509	17,7509	6 hours	0
			Total Duration 34,5 hours	Net Difference 0,0232(g)

Even though complex samples were aimed for cleaning, this sample still gives good insight in to the cleaning. The stainless steel metals A15 and A16 are identical in nature and the results (compared to stainless steel jacket) are much more promising as can be seen in the Table 9 & 10. The only difference was changing temperature settings to see how it is influenced by temperature changes. Generally, higher temperatures promote the efficiency of cleaning due to higher cavitation intensity, and heat eliminates entrapped air in the water.

Table 10: Ultrasonic cleaning of metal stainless steel A16

Clean Cycle (C)	Initial weight (g)	Weight after cleaning (g)	Duration	Difference (g)
C ₀	17,7406	17,7388	5,5 hours	0,0018
C ₁	17,7388	17,7384	5 hours	0,0004
C ₂	17,7384	17,7367	6 hours	0,0017
C ₃	17,7367	17,7364	7 hours	0,0003
C ₄	17,7366	17,7366	4 hours	0
			Total Duration 27,5 hours	Net Difference 0,0042(g)

As can be seen from the Table 9, the sample A15 loses a total of 3,7 mg at a total cumulative cleaning time of 28,5 hours, or the particles are removed at 0,13 mg/hour, whereas from the Table 10 the sample lost a total of 4,2 mg at a total cumulative cleaning time of 23,5 hours, or the particles are removed at 0,17 mg/hour.

Regardless of both samples being identically the same, the first metal plate sample (A15) was placed under normal operating conditions for cleaning(no heat addition via temperature knob ($T_{bath} = 0^{\circ}C$)). The second metal plate sample (A16) was cleaned at $T_{bath} = 60^{\circ}C$. This was done to see whether additional heat improves the efficiency of cleaning. It can be seen that the total cleaning time for A16 has been reduced by 5 hours.

It can be thus concluded that ultrasound does in fact promote particle removal. Higher temperatures reduce the cleaning time. No damage to the sample can be seen. The individual samples have also been tested for 24 hours during one instance of cleaning cycle. Apart from discoloration of Aluminum pixel (AlSi10Mg), there was no apparent damage to the sample. Furthermore, tests have been done on conventionally produced metal samples to use it as a benchmark and check for corrosion.

The results of ultrasounds have been graphed in Figure 29.

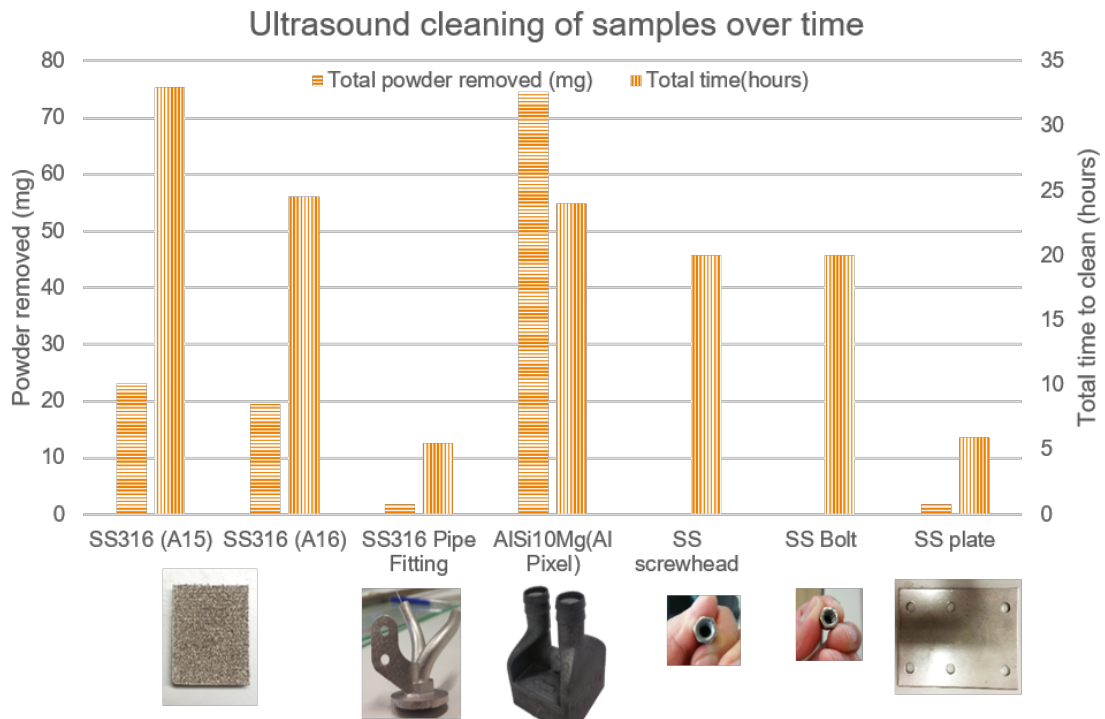


Figure 29: Total time and amount of particles removed per sample

In Figure 29, the amount of powder removed is represented by horizontal pattern bars whereas the the vertical pattern bars represent the total time it takes to clean the samples. In addition, the 3D printed samples have been graphed first followed by conventionally manufactured samples.the 3D printed samples have been graphed first followed by conventionally manufactured samples.

It must be mentioned that even though the conventional manufactured samples did not lose weight, it simply projects how long it had been under ultrasound exposure. From Figure 29, it can be seen that A15 took the longest time to clean. Comparing A15 with A16, it took 6 hours less to clean. This is due to the fact that A16 was cleaned at higher temperature. The least amount of hours taken to clean was by stainless steel pipe fitting. The Aluminum pixel lost the most weight. More complex the shape is, the more difficult it is to depowder. It can be concluded that the samples have been cleaned to great degree. However, it must be stated again that these samples are not freshly printed. Tests still need to be done with freshly printed metal parts to compare how the freshly printed structures perform.

Care should be exercised when the experiments are performed. According to material safety data sheet (MSDS) of stainless steel powder from the manufacturer, stainless steel powder is considered hazardous material that can pose serious risk to life. Furthermore, if the water is not regulated in the ultrasound bath, the experiment will run at infinite time until it either becomes non-operational or causes serious damage in its surroundings. To account for this, the experiment was conducted in Fume hood at all times, and 24 hour setup was devised.

The initial series of test on stainless steel cooling jacket were not that successful. In the sense

that even after exposing it to more than 30 hours of accumulative cleaning, it still lost weight. This was a concern since the sample is quite simple in design, having no internal dead spaces. To understand the reason, the sample was studied at the microscopic level. It was found that the structure is full of voids, cracks and the packing density is extremely poor. Thus, the particles that were loosely attached with the internal wall, could have easily become detached during the cleaning process. This material was then replaced with "state-of-the-art" printed stainless steel metal plate, and the results proved to be better in outcome.

5.4 Equipment for Imaging

To investigate the materials at microscopic level, light microscopy, SEM imaging and acoustic imaging were done. The equipment is available in TNO. The analysis provided great insight into material properties.

5.4.1 Light Microscopy

The Light Microscope at TNO, as can be seen in the Figure 30 uses a system of lenses and visible light to produce magnified images of small samples. Olympus KL 1500LCD acts as the light source for the microscope. Images under the microscope can be magnified from 8x-56x.



(a) SZX7 Zoom Stereo Microscope



(b) Olympus KL 1500LCD Light Source

Figure 30: Optical Light Microscope

5.4.2 Scanning Electron Microscope

Another equipment available at TNO is the Quanta 600 Scanning Electron Microscopy (SEM). The instrument requires an expert to operate for which help of Margo Segers was taken. The material is placed inside a vacuum chamber of the SEM. The instrument can magnify from 100x to 1000x.



Figure 31: Quanta 600 Scanning Electron Microscopy

5.4.3 Acoustic Imaging

Material inspection can also be done on layer-by-layer level by a far more advanced and robust microscope instrument, the Sonic ECHO™ scanning acoustic microscope. The instrument also requires an expert to operate, and help of Dr. Fischer was taken. The microscope can provide great in-depth properties of the material.



Figure 32: Sonix ECHO™

Stainless steel powder was inspected using the SEM magnified images by 1000x. This can be seen in Figure 33 where the powder is spherical in nature.

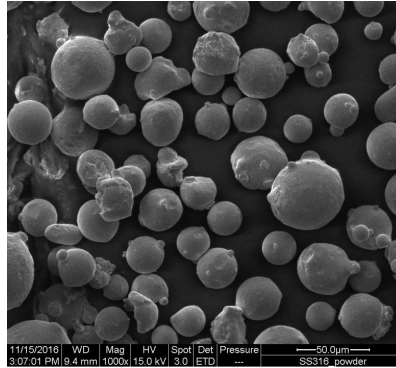


Figure 33: Scanning Electron Microscopy of stainless steel 316L powder 1000x magnification

The SEM image of stainless steel jacket can be seen in Figure 34. From the image it can be seen that the particles are not sintered well to each other. Gaps and voids can be seen and it appears that the particles are on top of each other rather than besides each other. Since the particles can be clearly designated, it means the original particle grains were not completely molten during the 3D printing. This can be seen in Figure 34. Thus it can be explained why the sample kept losing powder. The powders that appear to be on top of each other must be loosely adhered and hence are relatively easy to remove under ultrasonic cleaning.

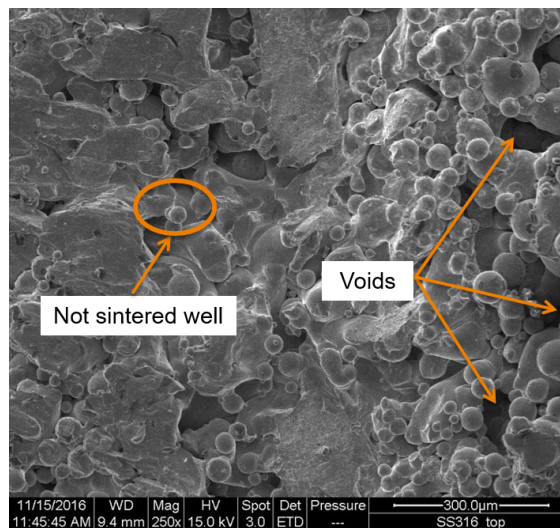
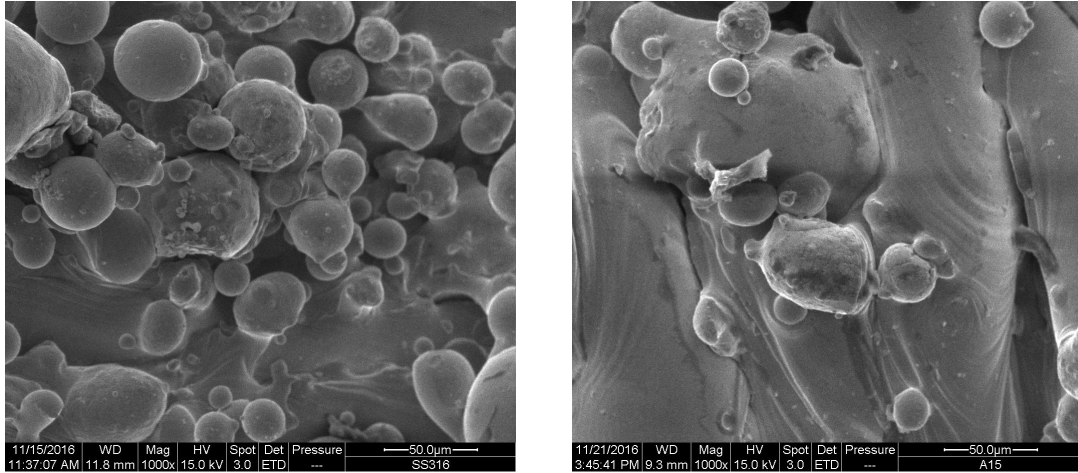


Figure 34: SEM of stainless steel cooling jacket 250x magnification

Compared to the stainless steel plate (A15), the particles can be seen better adhered to the surface. The packing density is good and minimum voids are observed. This can be seen in Figures 35a and 35b. It can also be seen that the particles are much better molten and layered within the sample of A15 compared to prominent visible particles in the stainless steel cooling jacket. The reason the particles are more visible in the stainless steel cooling jacket compared to

A15 is the fact that it was manufactured when research on ideal conditions for well sintered 3D samples during printing was ongoing.



(a) 1000x magnification of cooling jacket

(b) 1000x magnification of A15 metal plate

Figure 35: SEM of stainless steel cooling jacket and A15

5.5 Measuring angle of repose

5.5.1 Angle Of Repose

Angle of repose is the angle at which the powder rests at a steep angle and is at stable condition where no slipping occurs. Stainless steel powder is poured from a beaker to the filter where the powder flows steadily in large volumes. The angle of repose is calculated from Equation 5.2.

$$\tan\theta^0 = \frac{\text{height}}{\text{radius}} \quad (5.2)$$

where the height is the height of the cone of powder and the radius refers to half the diameter of the cone. The height of the cone is measured. Such experiment indicates that the powder is stable at angle 25°.

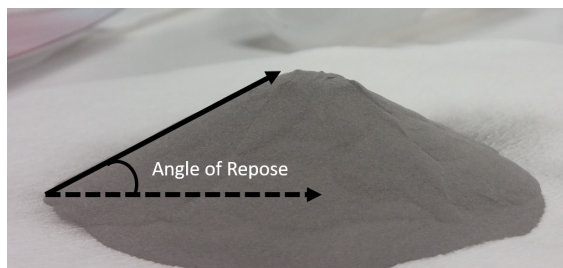


Figure 36: Measuring the height

6 Discussion and Conclusion

High quality parts with high level of clean complex 3D printed structures are not only a demand, but also a requirement in terms of practicality and feasibility. The main aim of the internship was to determine whether a 3D printed structure/sample can be depowdered. Depowdering is necessary if the final printed sample needs to be used in industrial applications. A powder filled sample will lead to poor functionality and may even cause contamination if the sample loses particle to its surroundings.

Two approaches to depowder such sample were considered in this internship. The first approach involved performing experiments where the sample is rotated under different angle orientations. The experiments are done to compare the results of depowdering simulation.

An experiment is carried out for determining ideal orientation where most depowdering occurs. The experiment is rotated either CCW or CW. It was interesting to see from the experimental and simulated results that the sample depowdered have different results.

While the simulation succeeded with depowdering the sample, the experiments indicated otherwise. This is explained by the fact that the simulation model considers ideal behavior of the powder where factors such as friction, interlocking, and real flow behavior are neglected. In addition, the model starts with a 100% powder filled sample compared to 53% actual powder filled in the experiments which is due to the complex nature of the sample. Unfortunately, the sample did not depowder completely. According to the simulation, the sample depowdered 99% and 89% in the CW and CCW direction respectively, whereas in the experiment the sample depowdered by 18% and 23% in the CW and CCW direction respectively. Tapping was also applied in one instance of the experiment. It could be seen the sample depowdered by 27%.

As a consequence, second approach for depowdering was needed where current available cleaning techniques are considered. These are namely Laser shockwave cleaning, chemical flushing, vibrations and gravity, electromagnetism and finally ultrasonic cleaning. Studying all the techniques intensively is tedious and thus out of all the available techniques, the technique which shows most promise and potential in regards to the limited time frame of internship is prioritized. Thus, ultrasonic cleaning is chosen. The experiments in fact showed that the sample can be completely cleaned. Moreover, the samples can be safely used unless they are to be used in an environment similar to rigorous conditions under the effect of ultrasonic waves.

During ultrasonic cleaning, experiments have been checked for any possibilities of corrosion. This was done by testing conventionally manufactured steel parts. The experiment shows no sign of corrosion.

The samples have also been investigated for material properties. Light Microscopy, Scanning Electron Microscopy and Acoustic Imaging have been done to shed some light into the material's properties. Under the SEM imaging the metal stainless steel cooling jacket shows poor mechanical properties. There seem to be large voids and there is non-uniform density packing. Individual particle grains are visible indicating poor sintering by laser of SLM. The sample was then replaced

by two stainless steel metal plates, A15 and A16. The results for cleaning improved since these samples had better mechanical properties and better density packing.

Furthermore, it was noted during the experiments that combination of different techniques improved the cleaning results. For instance, after the two approaches to depowdering, the aluminum pixel was refilled with powder again. Violent tapping and vibrations are applied to the sample which removed powder by 98%. Flushing it through water and then placing it again in ultrasonic bath removed the entire powder. This is observed when the final weight of the aluminum pixel matched the final weight of the aluminum pixel found via initial ultrasonic cleaning.

To conclude, the best method to depowder is via combination of techniques. An ideal approach to depowder the sample would be through consecutive methods (for instance, vibrations and gravity, then chemical flushing and final cleaning under ultrasounds) of cleaning. Not only will it reduce the cleaning hours required under ultrasonic cleaning but will ensure a complete depowdered sample.

7 Recommendations

Different techniques to obtain optimum method for depowdering, for e.g. LSC, chemical flushing and electromagnetism, should be investigated. The simulations for depowdering under different orientations provide useful information it still needs some improvements. The experimental and simulated results can be greatly improved by considering the following:

- Implement real behavior of power flow (namely interlocking, friction and roughness).
- Improving the experimental setup.
 - During rotation friction is prominent. Using frictionless bearing could improve the setup.
 - Experiment samples with simple internal geometries
 - Experiment with freshly 3D printed samples.
 - Use external excitation.
- Incorporating excitations in the depowdering model.

With regards to ultrasonic cleaning, further investigation is needed in:

- How sample properties, shapes and geometries, build-orientation is influenced under ultrasonic cleaning.
- Cleaning experiments with freshly 3D printed samples
- Samples of different material build.

Last but not the least, cleaning sequences could be inter-changed to see whether the order in which cleaning is done produces more efficient depowdering.

References

- BRITANNICA, ENCYCLOPEDIA 2017 Selective laser sintering. <https://www.britannica.com/topic/selective-laser-sintering>, visited on 14/12/16.
- DUNBAR, THOMAS, MAYNARD, BRIAN, THOMAS, DEREK A, PERI, MD MURTHY, VARGHESE, IVIN & CETINKAYA, CETIN 2007 Pressure amplification of laser induced plasma shockwaves with shock tubes for nanoparticle removal. *Journal of adhesion science and technology* **21** (1), 67–80.
- LAMMERS, NA, BLEEKER, IR A & VAN DER MULLEN, JJAM 2008 Laser shockwave cleaning .
- MITTAL, KASHMIRI LAL & JAISWAL, RAVI 2015 *Particle adhesion and removal*. John Wiley & Sons.
- QI, QUAN & BRERETON, GILES JOHN 1995 Mechanisms of removal of micron-sized particles by high-frequency ultrasonic waves. *IEEE transactions on ultrasonics, ferroelectrics, and frequency control* **42** (4), 619–629.
- VISSER, J 1995 Particle adhesion and removal: a review. *Particulate science and technology* **13** (3-4), 169–196.

8 Appendice

Appendix A Equipment Used

The following equipment's are used perform experiments.

Measuring scale

Table A.1: Mettler Toledo XS 104 Specs

Maximum capacity	<i>120 g</i>
Readability	<i>0.1 mg</i>
Minimum Weight (USP) Typical	<i>82 mg</i>
Dimensions (DxHxW)	<i>453 mm x 322 mm x 263 mm</i>
Settling Time	<i>1,5 s</i>
Weighing Pan Dimensions (WxD)	<i>73 mm x 78 mm</i>
Reproducibility (standard deviation)	<i>0,04 mg</i>

Table A.2: Mettler Toledo AE 160 Specs

Maximum capacity	<i>160 g</i>
Readability	<i>0.1 mg</i>
Weight Chamber Dimensions (WxDxH)	<i>172 mm x 155 mm x 220mm</i>
Balance housing (WxDxH)	<i>205 mm x 410 mm x 290 mm</i>
Settling Time	<i>5 s</i>
Weighing Pan Dimensions (Dia)	<i>Ø80mm</i>
Reproducibility (standard deviation)	<i>0,1 mg</i>

Oven

Table A.3: Heraeus T6120 Oven

Voltage	<i>220 V / 50 Hz</i>
Current	<i>6,5 A / 1,4 kW</i>
Nominal Temperature	<i>300 °C</i>
Operating Temperature	<i>150 °C</i>

Ultrasonic Bath

Table A.4: Bransonic Ultrasound RK 255 H

Maximum Capacity	<i>5,5 l</i>
Maximum Capacity (for cleaning)	<i>3,8 l</i>
Frequency (automatic frequency control)	<i>35 kHz</i>
Interior Dimensions (LxWxD)	<i>300 x 150 x 150 mm</i>
Ultrasonic peak output	<i>640 W</i>

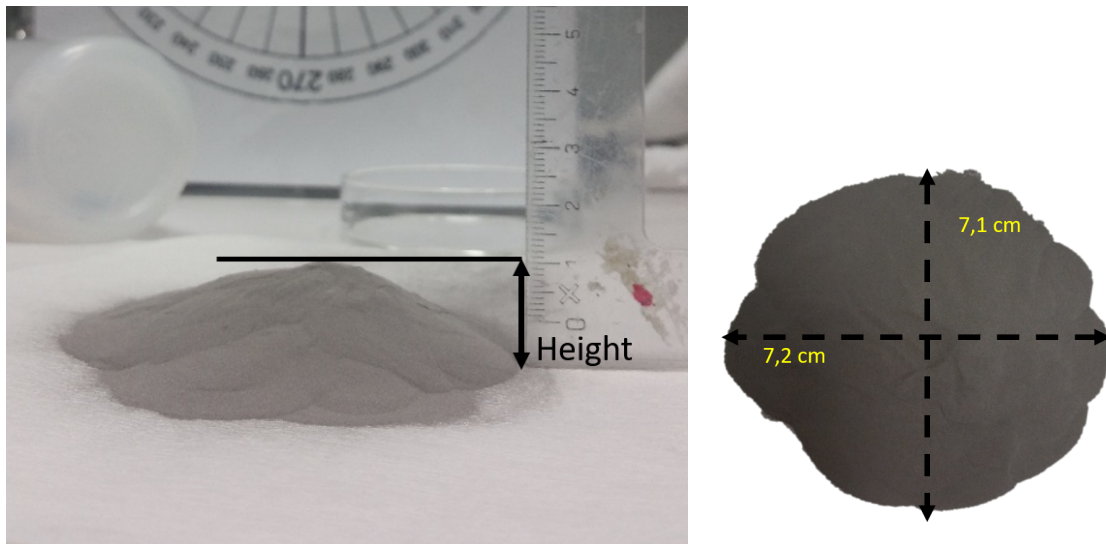
Non-Destructive Testing (NDT)

Table A.5: Sonix Echo

Maximum Capacity	<i>5,5 l</i>
Maximum Capacity (for cleaning)	<i>3,8 l</i>
Frequency (automatic frequency control)	<i>35 kHz</i>
Interior Dimensions (LxWxD)	<i>300 x 150 x 150 mm</i>
Ultrasonic peak output	<i>640 W</i>

Appendix B Measuring angle of repose

Stainless steel powder flows out a beaker and forms a cone as shown in Figure B.1. The height of the pile formed is measured using a ruler. The diameter of the pile of the powder is also measured, as can be seen in Figure B.1b. The mean of the two diameters are taken.



(a) Angle of repose.

(b) Diameter.

Figure B.1: Angle of repose.

Table B.6: Angle of repose

Height (cm)	Radius (cm)	Angle (θ°)
1,80	4,02	24,12
1,70	3,50	25,91
1,70	3,63	25,09

In order to calculate the angle of repose, the Equation 5.2 is used. The experiment has been repeated three times for an average angle of repose of 25° .